

## Quantitative Measurement of the Magnetic Exchange Interaction across a Vacuum Gap

R. Schmidt,<sup>1</sup> C. Lazo,<sup>2</sup> U. Kaiser,<sup>1</sup> A. Schwarz,<sup>1,\*</sup> S. Heinze,<sup>2</sup> and R. Wiesendanger<sup>1</sup>

<sup>1</sup>*Institute of Applied Physics, University of Hamburg, Jungiusstrasse 11, 20355 Hamburg, Germany*

<sup>2</sup>*Institute of Theoretical Physics and Astrophysics, University of Kiel, Leibnizstrasse 15, 24098 Kiel, Germany*

(Received 10 August 2010; revised manuscript received 11 March 2011; published 24 June 2011)

We demonstrate that magnetic exchange force spectroscopy allows for a quantitative determination of the distance-dependent magnetic exchange interaction across a vacuum gap. Experiments were performed on the antiferromagnetic Fe monolayer on W(001) with magnetically sensitive tips and compared to first-principles calculations performed for different cluster tip models. For stable tips, which can be distinguished from unstable tips by analyzing the dissipation signal, very good agreement with theory is observed.

DOI: [10.1103/PhysRevLett.106.257202](https://doi.org/10.1103/PhysRevLett.106.257202)

PACS numbers: 75.30.Et, 68.37.Ps, 75.70.Ak

Properties of magnetic materials are governed by the magnetic exchange interaction between individual atomic magnetic moments (spins). A concept often used to describe the interaction between two spins  $\mathbf{S}_1$  and  $\mathbf{S}_2$  is the Heisenberg model, i.e.,  $H = -J\mathbf{S}_1\mathbf{S}_2$ , where  $J$  is the exchange constant. Its sign determines, whether a parallel (ferromagnetic) or antiparallel (antiferromagnetic) alignment between the atomic magnetic moments is preferred. In solids a variety of very different coupling mechanisms are observed, e.g., direct exchange, superexchange or double exchange across nonmagnetic bridging atoms as well as indirect coupling between localized spins in itinerant metals via polarization of the conduction electrons. In the latter case, an oscillatory Ruderman-Kittel-Kasuya-Yoshida (RKKY) behavior is expected, where the sign of  $J$  changes with distance. A change of sign can also occur, if only direct exchange between overlapping  $d$  orbitals in transition metals is considered as in the Bethe-Slater curve or discussed by Moriya [1] based on the Alexander-Anderson model [2].

Experimentally, it is rather difficult to measure the distance dependence of the magnetic exchange interaction between two magnetic atoms. Recently, the oscillatory RKKY-type magnetic exchange interaction between pairs of individual Co adatoms has been measured employing scanning tunneling microscopy (STM) on Cu(111) by evaluating the Kondo resonance [3] and on Pt(111) by analyzing magnetization curves recorded with spin-polarized STM (SP-STM) [4]. In both cases the magnetic coupling is mediated via conduction electrons of the nonmagnetic substrate. Up to now magnetic exchange interactions across a vacuum gap were only considered theoretically utilizing density functional theory (DFT) [5–9].

In this Letter we employed magnetic exchange force microscopy (MExFM) [8,10] in its spectroscopic mode (magnetic exchange force spectroscopy: MExFS), to quantitatively measure the distance dependence of the magnetic exchange energy  $E_{\text{ex}}(z)$  across the vacuum gap between an atomically sharp magnetically sensitive tip and the

antiferromagnetically ordered Fe monolayer on W(001). The simultaneously recorded energy dissipation  $E_{\text{D}}(z)$  allows the identification of nondissipative and hence stable tips. For such tips  $E_{\text{ex}}(z)$  can be elegantly obtained by subtracting distance-dependent curves recorded on Fe atoms with oppositely oriented spins, whereby all nonmagnetic contributions are eliminated. The results are compared to first-principles DFT calculations performed for different pyramidal cluster tips. They reveal that antiferromagnetic coupling is always favored at short distances ( $< 370$  pm) and that the magnitude is on the order of 100 meV. Regarding magnitude and distance dependence, very good agreement is obtained with experimental data recorded with a stable tip. Moreover, we argue that dissipative tips cannot be analyzed this way, as they change, depending on tip-sample distance, their atomic structure.

The experiments have been carried out in ultrahigh vacuum at 8.1 K with a home built atomic force microscopy setup (*Hamburg design*) equipped with a 5 T superconducting magnet [11]. Si cantilevers were coated *in situ* with a few nm Cr to obtain magnetically sensitive force sensors. As a sample we selected the Fe monolayer on W(001), which grows pseudomorphically and exhibits an antiferromagnetic spin structure with out-of-plane anisotropy [12]. Data acquisition was performed in the dynamic mode using the frequency modulation technique while keeping the oscillation amplitude  $A$  constant [13]. Imaging is done in the noncontact regime at a constant frequency shift  $\Delta f(z)$ . In the spectroscopy mode  $\Delta f(z)$  curves are recorded, which can be converted into  $E(z)$  curves using well established numerical algorithms [14–16]. Taking a spectroscopy curve at every  $(x, y)$  image point is known as three-dimensional force field spectroscopy (3D-FFS) [17]. In all cases the excitation amplitude  $a_{\text{exc}}$  required to keep  $A$  constant is recorded as well and used to calculate the dissipated energy  $E_{\text{D}}$ . More details regarding experimental procedures, data acquisition parameters, and conversion procedures are described in the supplemental material [18].

An overview image of the sample topography is displayed in Fig. 1(a). In (b) an atomically resolved image across a step between monolayer and double layer is shown. The  $c(2 \times 2)$  pattern on the monolayer reflects its antiferromagnetic structure and proves that the tip is magnetically sensitive [8]. As-prepared Cr-coated tips usually do not exhibit magnetic sensitivity, even if an external magnetic field normal to the surface, i.e., collinear to the spin orientation at the surface, is applied [19]. Therefore, slight tip modifications are intentionally induced, e.g., by scanning across a step edge on the sample surface at closer and closer tip-sample distances, until the tip becomes magnetically sensitive. During this procedure, Fe might be picked up eventually. Thus, the initially Cr-coated tip is either Cr or Fe terminated afterwards. With such a magnetically sensitive tip, 3D magnetic exchange force spectroscopy (3D-MExFS) data sets are recorded in one of the two methods described in the supplemental material [18]. Figure 1(c) shows such an atomically resolved data set. Note that a larger attractive tip-sample interaction (larger negative  $\Delta f$ ; see slice along the [100]-direction) corresponds to maxima in constant  $\Delta f$  images (see bottom image).

Based on such a 3D-MExFS data set individual  $\Delta f(z)$  curves on surface atoms with oppositely oriented spins can be unambiguously identified. They are displayed in Figs. 2

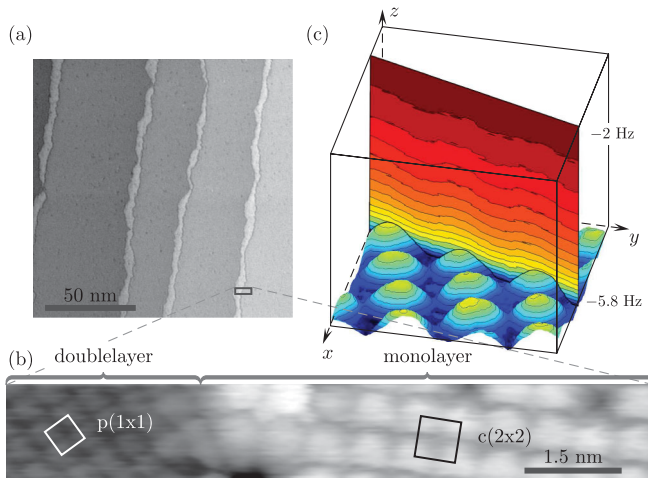


FIG. 1 (color). (a) Topography of 1.1 atomic layers of Fe deposited on W(001). (b) Atomically resolved image across a step between the ferromagnetic double layer (left) and the antiferromagnetic monolayer (right). The  $c(2 \times 2)$  pattern on the monolayer proves that the tip is magnetically sensitive [8]. (c) Atomically resolved 3D-MExFS data obtained on the Fe monolayer. Sites with opposite spin orientations can be identified as maxima and minima in the topographic data at the bottom. The color coded slice through the  $\Delta f(x, y, z)$  data set along the [100]-direction reflects the site and distance dependence of the magnetic exchange interaction. Parameters:  $T = 8.1$  K,  $B = 5$  T,  $f_0 = 187$  kHz,  $A = 3.83$  nm,  $c_z = 145.5$  N/m,  $\Delta f_{\text{stab}} = -5.8$  Hz,  $x \times y \times z = 1.5$  nm  $\times$  1.5 nm  $\times$  0.3 nm ( $32 \times 32 \times 256$  pts.).

and 3 for two different experiments performed with a nondissipative and a dissipative tip, respectively (see lower curves, in which  $E_D$  is plotted relative to the intrinsic dissipation). The insets show the atomically spin-resolved images recorded with the corresponding tips. No absolute  $z$  scale can be extracted from experimental data; i.e.,  $z = 0$  pm is arbitrarily set at the closest tip-sample distance.

The stable tip (Fig. 2) shows two smooth  $\Delta f(z)$  curves, which are indistinguishable at larger distances, but split into two branches at smaller distances. Both  $\Delta f(z)$  curves represent the total tip-sample interaction. Since all nonmagnetic contributions such as the long-range van der Waals interaction as well as the short-range chemical interaction are identical on both sites of opposite spin orientation, the frequency shift  $\Delta f_{\text{ex}}(z)$  representing the magnetic exchange interaction can be extracted simply by subtracting the curves from each other, i.e.,  $\Delta f_{\text{ex}}(z) = \Delta f_{\text{max}}(z) - \Delta f_{\text{min}}(z)$  (black circles). Note that the relative spin orientation is not known *a priori*, but choosing the sign definition  $\Delta f_{\text{ex}}(z) = \Delta f_{\text{max}}(z) - \Delta f_{\text{min}}(z)$  is justified by comparison with theory (see below). For further quantitative comparison with theory,  $\Delta f_{\text{ex}}(z)$  can be converted into  $E_{\text{ex}}(z)$  (cf. Fig. 4).

In Fig. 3 both curves exhibit a sudden steep decrease of the  $\Delta f(z)$  curve at  $z$  positions separated by about 12 pm. At exactly the same positions the dissipation increases drastically to about 3 eV/cycle at the smallest separation. Such a large dissipation is usually associated with adhesion hysteresis [20–22], i.e., reversible reconfigurations of atoms at

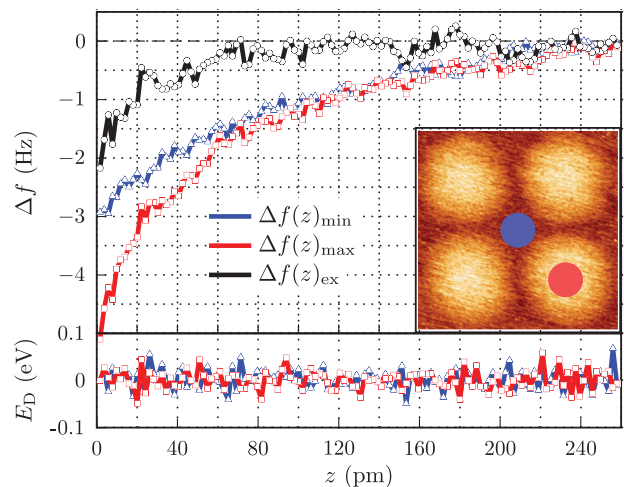


FIG. 2 (color). Two individual  $\Delta f(z)$  curves recorded with a nondissipative ( $E_D(z) = \text{const}$ ; see bottom curve) and hence stable tip on Fe atoms with opposite spins. Both curves split smoothly into two branches at small tip-sample distances. The difference between both curves (black circles) is a measure of the magnetic exchange interaction and can be converted into  $E_{\text{ex}}(z)$ ; cf. Fig. 4. The inset shows the smooth MExFM image recorded with the same stable nondissipative tip. Parameters:  $T = 8.1$  K,  $B = 5$  T,  $f_0 = 187$  kHz,  $A = 3.83$  nm,  $c_z = 145.5$  N/m,  $\Delta f_{\text{stab}} = -2.5$  Hz,  $\Delta z = 2$  pm.

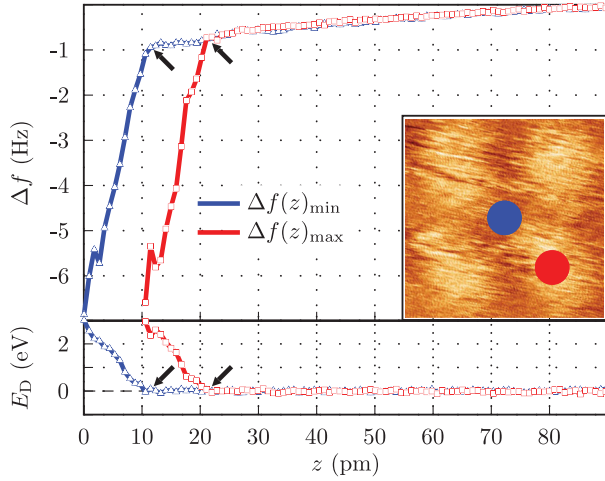


FIG. 3 (color). Two individual  $\Delta f(z)$  curves recorded with a dissipative tip (see bottom curve) on Fe atoms with opposite spins. Both curves exhibit a sudden steep decrease at a certain tip-sample distance separated by about 12 pm that coincides with a sudden increase in dissipated energy (see arrows). Such features suggest atomic reconfigurations at the tip apex. Hence,  $E_{\text{ex}}(z)$  cannot be extracted by subtracting both curves from each other. The MExFM image recorded with the same tip (see inset) exhibits a larger noise level than in Fig. 2 recorded with a stable nondissipative tip. Parameters:  $T = 8.1$  K,  $B = 5$  T,  $f_0 = 190$  kHz,  $A = 3.89$  nm,  $c_z = 151.0$  N/m,  $\Delta f_{\text{stab}} = -6.5$  Hz,  $\Delta z = 0.88$  pm.

the tip apex, which occur at different tip-sample distances during approach and retrace of an oscillation cycle [23]. Since the tip apex structure is different before and after the onset of dissipation,  $\Delta f_{\text{ex}}(z)$ , and hence  $E_{\text{ex}}(z)$ , cannot be extracted by subtracting both curves from each other, although the tip is magnetically sensitive as demonstrated by the MExFM image displayed in the inset. Furthermore, this MExFM image exhibits more noise than the MExFM image obtained with a stable tip in Fig. 2. Indeed, evaluating six 3D-MExFS data sets and more than 20 MExFM images shows that the features in the spectroscopy curves and image data as found in Figs. 2 and 3, respectively, are characteristic for nondissipative (stable) and dissipative (unstable) tips.

In order to interpret the experimentally obtained  $E_{\text{ex}}(z)$  curves, we have performed DFT based first-principles calculations within the generalized gradient approximation [24] to the exchange-correlation potential. We apply the full-potential linearized augmented plane wave method as implemented in the WIEN2K [25] code. The energy cutoff for the plane wave representation in the interstitial region is  $E_{\text{max}}^{\text{wf}} = 13$  Ry and a  $(3 \times 3 \times 1)$  Monkhorst-Pack grid was used for the Brillouin zone integration. The coupled system of tip and sample was calculated in a supercell geometry as described in Ref. [7]. The Fe monolayer on W(001) was modeled by a symmetric slab with five W layers and one Fe layer on each side. Four different pyramidal three layer tips consisting of 14 atoms were considered (see sketches in

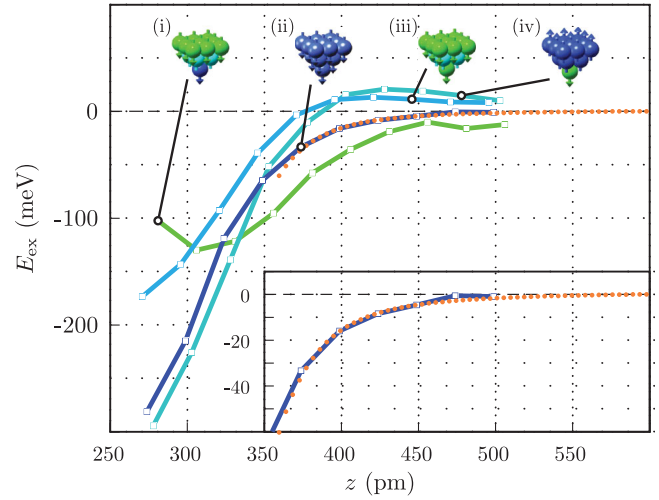


FIG. 4 (color). Comparison between theoretical and experimental  $E_{\text{ex}}(z)$  curves.  $E_{\text{ex}}(z)$  with the Fe-ML on W(001) was calculated using DFT for four different tips. Chemical composition (blue: Fe; green/cyan: Cr) and spin structure are indicated for each curve.  $E_{\text{ex}} > 0$  ( $E_{\text{ex}} < 0$ ) indicates a ferromagnetic (antiferromagnetic) coupling.  $E_{\text{ex}}(z)$  obtained with the nondissipative tip (cf. Fig. 2) is plotted as well (orange curve) [26]. It fits very well with the theoretical result for a pure Fe tip apex (see inset).

Fig. 4): (i) a Cr-base with an Fe termination, (ii) a pure Fe tip, (iii) a pure Cr tip, and (iv) an Fe-base with a Cr termination. These choices reflect possible tip configurations, which could occur after the deliberately induced collision between the Cr-coated tips and the Fe monolayer described above. Note that adjacent Cr layers as well as adjacent Fe and Cr layers are coupled antiferromagnetically, while coupling in the pure Fe tip is ferromagnetic. Tip and surface were relaxed independently before considering the coupled system. The tip was then approached towards the surface along a trajectory of discrete points. For every distance, we carried out a DFT calculation including structural relaxations of the tip atoms and the Fe monolayer and uppermost W layer. As in the experimental situation, the separation  $z$  in the coupled system is defined as the distance between the tip apex atom and the Fe surface atom before considering relaxations. While approaching the different tip models towards the surface, no structural reconfigurations of the tip apices were observed. Thus, our tip models reflect stable nondissipative tips.

For every tip we considered a parallel (P) and an anti-parallel (AP) alignment of the magnetic moments of the tip apex atom and the surface atom underneath. Relaxations on the order of 10 pm were observed for all tips, but no reconfigurations or instabilities. The magnetic exchange energy  $E_{\text{ex}}(z)$  is obtained by subtracting the total energies in the AP and P alignment, i.e.,  $E_{\text{ex}}(z) = E_{\text{AP}}(z) - E_{\text{P}}(z)$ .  $E_{\text{ex}}(z) > 0$  ( $< 0$ ) indicates ferromagnetic (antiferromagnetic) coupling. This approach is equivalent to subtracting

the experimental data obtained on minima and maxima as performed for the stable nondissipative tip. Because of reconfigurations at the tip apex, a direct comparison of the data recorded with dissipative tips is not possible. Note that the tips used for the calculations are much smaller than real tips and long-range interactions are not accounted for. However, after subtraction all nonmagnetic contributions to the total tip-sample interaction cancel out.

The calculated  $E_{\text{ex}}(z)$  curves are displayed in Fig. 4. At small tip-sample distances  $E_{\text{ex}}$  is negative indicating the favorable antiferromagnetic exchange interaction in accordance with the simple Bethe-Slater picture of direct exchange. This finding justifies the sign definition of  $\Delta f_{\text{ex}}(z)$  used for the experimental data. The magnitude at a distance of 300–350 pm, is antiferromagnetic and on the order of 100 meV. Interestingly, only Cr-terminated tips show a characteristic change of sign at large distances due to a transition from a direct to an indirect exchange mechanism [9].

For direct comparison between theoretical predictions and experimental data,  $E_{\text{ex}}(z)$  obtained with the nondissipative stable tip is displayed in Fig. 4 as well. Since no sign change is observed in the experimental data, we can infer that the tip is Fe terminated (only Cr-terminated tips exhibit a sign change), most probably because the Cr-coated tip picks up surface Fe atoms during our tip-preparation procedure. Since we never observed a sign reversal up to now, our tip-preparation procedure seems to favor Fe-terminated tip apices. In the experiment, the absolute  $z$  position is not known. Therefore, we shifted the experimental curve in  $z$  direction with respect to the theoretical curves. Best agreement between theory and experiment is found for the pure Fe tip apex, for which magnitude as well as the distance dependence of the magnetic exchange energy fit very well as visible in the inset.

The exemplary result displayed in Figs. 2 and 4 demonstrates that our method enables us to quantitatively measure the magnetic exchange interaction across a vacuum gap. Both, distance dependence and magnitude can be accurately measured using stable and hence nondissipative tips. Unsuitable tips can be identified by analyzing the dissipation signal. Our experimental procedure can be universally applied to any combination of similar or dissimilar atomic species to measure the distance dependence of the magnetic exchange interaction across a vacuum gap with atomic resolution, even on insulating tip-sample systems. Moreover, our experiments suggest that the magnetic exchange interaction can be utilized to switch the magnetic state of atoms, clusters or molecules in a controlled fashion

by placing a magnetic tip in an MExFM or SP-STM setup lower than about 0.5 nm above the specimen.

We acknowledge financial support from the DFG (SFB 668-A5 and HE 3292/7-1), the ERC Advanced Grant FUIRORE, and from the Cluster of Excellence NANOSPINTRONICS.

\*Corresponding author.

aschwarz@physnet.uni-hamburg.de

- [1] T. Moriya, *Solid State Commun.* **2**, 239 (1964).
- [2] S. Alexander and P.W. Anderson, *Phys. Rev.* **133**, A1594 (1964).
- [3] P. Wahl *et al.*, *Phys. Rev. Lett.* **98**, 056601 (2007).
- [4] L. Zhou *et al.*, *Nature Phys.* **6**, 187 (2010).
- [5] A. S. Foster and A. L. Shluger, *Surf. Sci.* **490**, 211 (2001).
- [6] H. Momida and T. Oguchi, *Surf. Sci.* **590**, 42 (2005).
- [7] C. Lazo *et al.*, *Phys. Rev. B* **78**, 214416 (2008).
- [8] R. Schmidt *et al.*, *Nano Lett.* **9**, 200 (2009).
- [9] K. Tao *et al.*, *Phys. Rev. Lett.* **103**, 057202 (2009).
- [10] U. Kaiser, A. Schwarz, and R. Wiesendanger, *Nature (London)* **446**, 522 (2007).
- [11] M. Liebmann *et al.*, *Rev. Sci. Instrum.* **73**, 3508 (2002).
- [12] A. Kubetzka *et al.*, *Phys. Rev. Lett.* **94**, 087204 (2005).
- [13] T. R. Albrecht *et al.*, *J. Appl. Phys.* **69**, 668 (1991).
- [14] U. Dürig, *Appl. Phys. Lett.* **75**, 433 (1999).
- [15] F. J. Giessibl, *Appl. Phys. Lett.* **78**, 123 (2001).
- [16] J. Sader and S. P. Jarvis, *Appl. Phys. Lett.* **84**, 1801 (2004).
- [17] H. Hölscher *et al.*, *Appl. Phys. Lett.* **81**, 4428 (2002).
- [18] See supplemental material at <http://link.aps.org/supplemental/10.1103/PhysRevLett.106.257202> for details regarding experimental and theoretical aspects.
- [19] Compared to typical interatomic magnetic exchange energies the Zeeman energy of 5 T is negligible and should not alter the distance dependence.
- [20] N. Sasaki and M. Tsukada, *Jpn. J. Appl. Phys.* **39**, L1334 (2000).
- [21] T. Trevelyan and L. Kantorovich, *Nanotechnology* **15**, S34 (2004).
- [22] S. A. Ghasemi *et al.*, *Phys. Rev. Lett.* **100**, 236106 (2008).
- [23] Noteworthy, calculations revealed that the magnetic exchange interactions contribute to relaxation effects [7] and it is hence likely that they contribute to dissipative reconfigurations as well.
- [24] J. P. Perdew, K. Burke, and M. Ernzerhof, *Phys. Rev. Lett.* **77**, 3865 (1996).
- [25] K. Schwarz, P. Blaha, and G. K. H. Madsen, *Comput. Phys. Commun.* **147**, 71 (2002).
- [26] Several curves recorded on minima and maxima from the same 3D-MExFS data are averaged to calculate  $E_{\text{ex}}(z)$ .